

Changes in Soil Hydraulic Properties Caused by Construction of a Simulated Waste Trench at the Idaho National Engineering Laboratory, Idaho

By Stephanie Shakofsky

U.S. GEOLOGICAL SURVEY

Water-Resources Investigations Report 95-4058

**Prepared in cooperation with the
U.S. DEPARTMENT OF ENERGY**

**Idaho Falls, Idaho
March 1995**



U.S. DEPARTMENT OF THE INTERIOR

BRUCE BABBITT, Secretary

U.S. GEOLOGICAL SURVEY

Gordon P. Eaton, Director

Any use of trade, product, or firm names is for descriptive purposes only and does not imply endorsement by the U.S. Government.

For additional information write to:

Project Chief
U.S. Geological Survey
INEL, MS 4148
P.O. Box 2230
Idaho Falls, ID 83403

Copies of this report can be purchased from:

U.S. Geological Survey
Earth Science Information Center
Open-File Reports Section
Box 25286, MS 517
Denver Federal Center
Denver, CO 80225

Contents

Abstract	1
Introduction	1
Purpose and scope	4
Geohydrologic setting	4
Methods	7
Physical properties of soil	10
Soil profile description	10
Aggregate distribution	10
Carbonate content	10
Particle-size analysis	13
Hydraulic properties of soil	13
Soil-moisture retention curves	13
Saturated hydraulic conductivity	13
Unsaturated hydraulic conductivity, $K(\theta)$	13
Differences in physical and hydraulic properties of disturbed and undisturbed sediments	13
Summary and conclusions	24
References	24

Illustrations

Figure 1. Map showing location of the Idaho National Engineering Laboratory and generalized direction of flow in the Snake River Plain aquifer	2
2. Map showing location of the Radioactive Waste Management Complex and USGS test trench area	3
3. Cross section of the simulated waste trench within the USGS test trench area, showing the excavated area and location of neutron-probe access holes	5
4. Geologic section showing subsurface geology at the Radioactive Waste Management Complex	6
5. Map showing location of the USGS test trench area, monitoring facilities, and soil-sample collection sites	8
6. Graph showing particle-size distribution with depth in the undisturbed area and the simulated waste trench at the USGS test trench area.	14
7. Graphs showing soil-moisture retention curves plotted by depth for sediment samples in the undisturbed area and simulated waste trench at the USGS test trench area	15
8. Graphs showing saturated hydraulic conductivity variation in the undisturbed area and the simulated waste trench with number of experimental runs, USGS test trench area	16
9. Graphs showing unsaturated hydraulic conductivity curves with saturated hydraulic conductivity, plotted by depth in the undisturbed area and the simulated waste trench at the USGS test trench area	17
10. Graphs showing composited distribution of soil properties in a silt loam soil for undisturbed and simulated waste trench profiles at the USGS test trench area	19
11. Graphs showing soil-moisture retention curves for disturbed and undisturbed soils at the simulated waste trench, USGS test trench area	21
12. Graphs showing frequency distribution of effective pore sizes in disturbed and undisturbed soils at the simulated waste trench, USGS test trench area	22

13. Graph showing K(θ) curves for disturbed and undisturbed soils at the simulated waste trench, USGS test trench area	23
---	----

Tables

Table 1. Soil profile description	11
2. Aggregate distribution	11
3. Reaction between soil and hydrochloric acid	12
4. Particle-size distribution by method	12
5. Summary of soil properties	18

Conversion Factors and Abbreviated Units

Multiply	By	To Obtain
millimeter (mm)	0.03937	inch
centimeter (cm)	0.3937	inch
meter (m)	3.281	foot
kilometer (km)	0.6214	mile
centimeter per second (cm/s)	0.03281	foot per second
centimeter of water (cm of water)	0.0142233	pound-force/square inch
square kilometer (km ²)	0.3861	square mile
cubic centimeter (cm ³)	0.06102	cubic inch
cubic meter (m ³)	35.31	cubic foot
gram (g)	0.002205	pound
kilogram (kg)	2.205	pound
gram per cubic centimeter (g/cm ³)	0.57801	ounce/cubic inch
milliNewton per meter (mN/m)	5.71 x 10 ⁻⁶	pound-force/inch

Temperature can be converted from degrees Celsius (°C) to degrees Fahrenheit (°F) by the equation:

$$^{\circ}\text{F} = (^{\circ}\text{C} \times 1.8) + 32$$

Abbreviated units used in report: mol/L (mole per liter)

Changes in Soil Hydraulic Properties Caused by Construction of a Simulated Waste Trench at the Idaho National Engineering Laboratory, Idaho

by Stephanie Shakofsky

Abstract

In order to assess the effect of filled waste disposal trenches on transport-governing soil properties, comparisons were made between profiles of undisturbed soil and disturbed soil in a simulated waste trench. The changes in soil properties induced by the construction of a simulated waste trench were measured near the Radioactive Waste Management Complex at the Idaho National Engineering Laboratory (INEL) in the semi-arid southeast region of Idaho. The soil samples were collected, using a hydraulically-driven sampler to minimize sample disruption, from both a simulated waste trench and an undisturbed area nearby. Results show that the undisturbed profile has distinct layers whose properties differ significantly, whereas the soil profile in the simulated waste trench is, by comparison, homogeneous. Porosity was increased in the disturbed cores, and, correspondingly, saturated hydraulic conductivities were on average three times higher. With higher soil-moisture contents (greater than 0.32), unsaturated hydraulic conductivities for the undisturbed cores were typically greater than those for the disturbed cores. With lower moisture contents, most of the disturbed cores had greater hydraulic conductivities. The observed differences in hydraulic conductivities are interpreted and discussed as changes in the soil pore geometry.

INTRODUCTION

The Idaho National Engineering Laboratory (INEL), established in 1949, is operated by the U.S. Department of Energy (DOE) primarily to build, operate, and test nuclear reactors. The INEL is

situated on the eastern Snake River Plain in southeastern Idaho and comprises approximately 2,300 km² (fig. 1).

The Radioactive Waste Management Complex (RWMC), located in the southwest corner of the INEL (fig. 2), was established in 1952 as a controlled area for the management of radioactive waste. The site is relatively level and is situated in a shallow topographic depression surrounded by low hills. Because the RWMC is in a topographic depression, the area is vulnerable to flooding, and has been flooded three times in the recent past (1962, 1969, and 1982) as a result of rapid spring snow melt.

Chemical, low-level radioactive, and trans-uranic radioactive wastes, mostly stored in 55-gallon drums, are buried in trenches and pits in the surficial sediments, about 3 to 6 m below the surface, at the Subsurface Disposal Area (SDA) within the RWMC. From 1952 to 1986, approximately 180,000 m³ of radioactive wastes, with a total activity of about 9.5 million curies of radioactivity, were buried at the SDA. Monitoring wells in and downgradient of the RWMC show that ground water has been contaminated by organic compounds (Laney and Minkin, 1988). Radionuclides have migrated from burial sites, and have been detected to a depth of about 34 m below the surface (Humphrey and others, 1982). A comprehensive study to determine the potential for future migration of radionuclides into the underlying Snake River Plain aquifer, which is approximately 180 m below the surface, has been undertaken by the United States Geological Survey (USGS) in cooperation with the DOE.

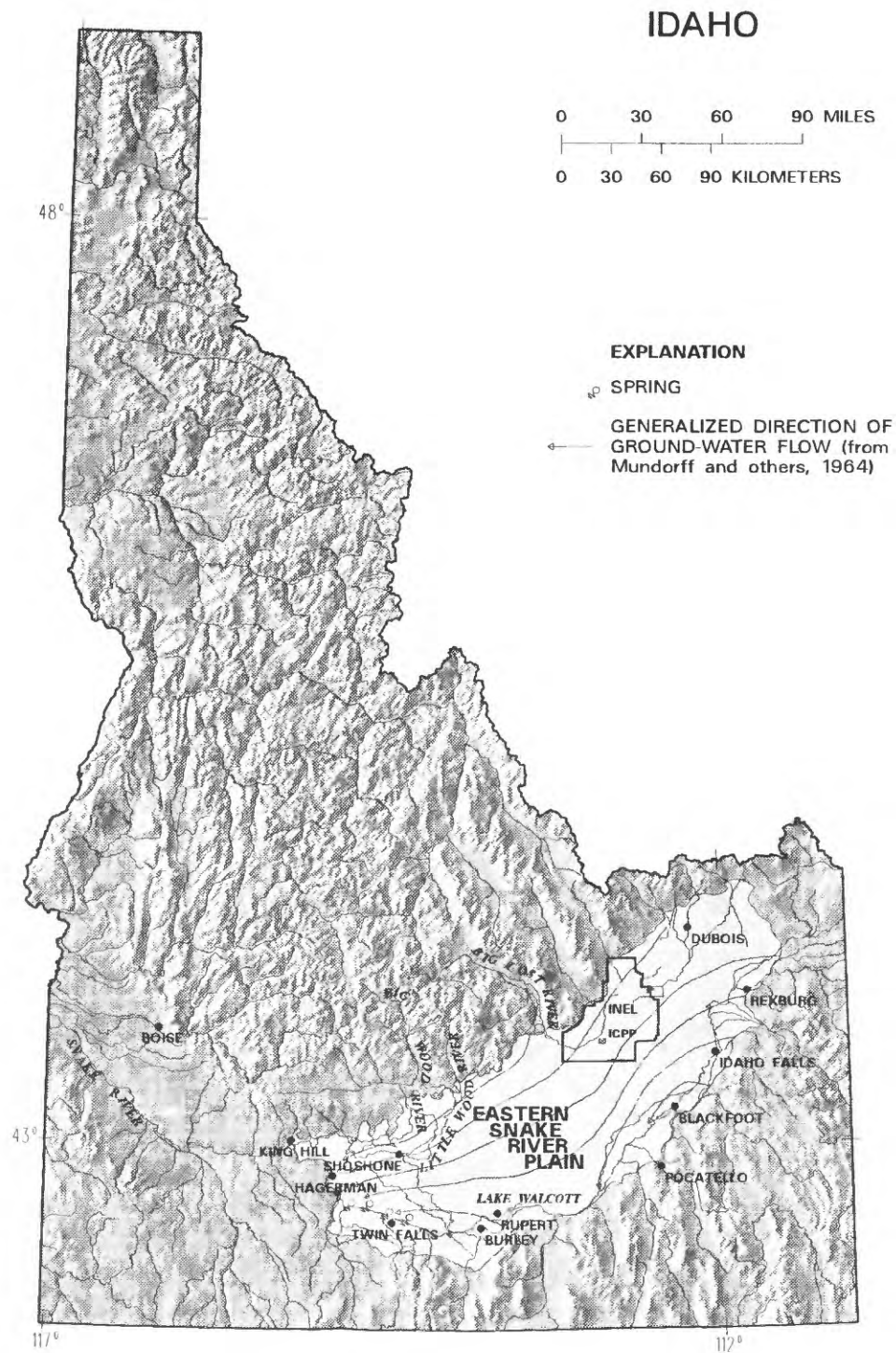


Figure 1. Location of the Idaho National Engineering Laboratory and generalized direction of flow in the Snake River Plain aquifer.

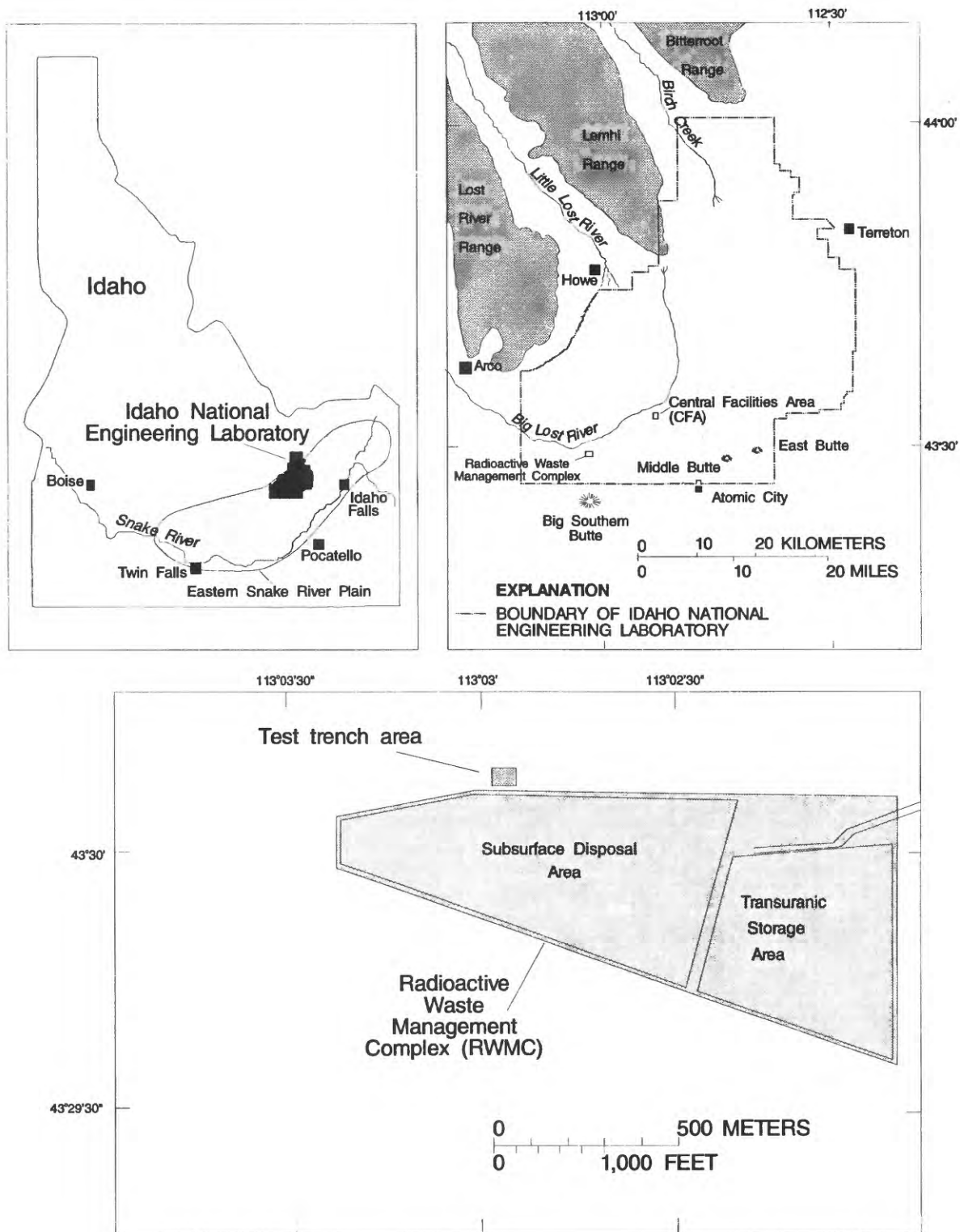


Figure 2. Location of the Radioactive Waste Management Complex and USGS test trench area.

Because hydrologic experimentation in the waste pits is potentially dangerous, the USGS in 1986 constructed a simulated waste trench in the USGS test trench area just north of the SDA boundary (Davis and Pittman, 1990). In constructing the simulated waste trench (fig. 3), an attempt was made to employ the method of waste burial historically practiced at the SDA. This practice involved excavating the trench to the top basalt layer (ranging between 3 to 6 m below the ground surface), emplacing the barrels, and backfilling the trench with the excavated soil. Neither compaction of soil nor capping of the trench were regular practices at the SDA.

Because the rate with which radionuclides migrate depends greatly on the amount of water reaching and passing through buried waste, the objective of the overall effort at the USGS test trench area was to model the SDA and to investigate water movement and transport through the unsaturated surficial sediments. The trench study was designed to obtain a reliable estimate of the quantity of water that infiltrates, comes in contact with the waste, and eventually recharges the aquifer in this area.

Purpose and Scope

This report compares the hydraulic characteristics of both the undisturbed soil profile and the disturbed soil of the simulated waste trench, focusing on the changes that occur when a soil is disturbed by the construction of a waste trench. Specifically, the texture, bulk density, porosity, and aggregation of an undisturbed and a disturbed soil and the effects of these properties on soil-moisture retention and hydraulic conductivities are examined.

Laboratory techniques were used on both a disturbed soil sample from the simulated waste trench and an undisturbed soil sample collected adjacent to the simulated waste trench to determine the effects of disturbance on soil hydraulic properties. This study determined the physical and hydraulic properties of minimally disrupted soil-core samples, including at least two each of disturbed and undisturbed samples from average depths of 18, 30, 80, 145, and 235 cm. To minimize disruption of the soil

sample in the laboratory, the hydraulic experiments were carried out with the sample remaining in its original soil ring (i.e. no recoring, repacking, or subsampling of the samples occurred).

Geohydrologic Setting

The INEL is bounded on the north and east by mountains of the Basin and Range province. For the most part, this area is sagebrush-covered and semi-arid. Based on National Oceanic and Atmospheric Administration (NOAA) records from 1950 to 1988 (Clawson and others, 1989), the area receives an average annual precipitation of 221 mm, with about 30 percent falling as snow. The annual precipitation at the RWMC for 1986 and 1987 was 240 mm and 175 mm, respectively. The average daily air temperature for 1987 at the USGS test trench ranged from 26.7 °C on August 6 to -14.6 °C on December 25 (Davis and Pittman, 1990).

The eastern Snake River Plain is a structural basin about 325 km long and 100 km wide, which is underlain by a sequence of basalt flows intercalated with thin sedimentary units (fig. 4). These flow units, in turn, are underlain by older rhyolitic rocks.

The RWMC is located in a shallow depression floored by basaltic lava flows and by wind- and water-deposited sediments. It is surrounded by hummocky basalt flows of low relief which control the thickness of the overlying surficial sediment. The surficial sediments consist of about 3 to 6 m of sand, silt, clay, and lesser amounts of gravel. The sediments are dominantly floodplain and wind-blown deposits. The floodplain deposits resulted from periodic Late Pleistocene and Holocene incursions of the Big Lost River into the area. Sediments from ephemeral lacustrine environments are also present (Rightmire and Lewis, 1987).

Stratigraphic relations in the unsaturated zone and uppermost part of the aquifer are the result of 10 major cycles of volcanism and sediment deposition during the past 600,000 years. Brief volcanic eruptions from at least 10 different source vents resulted in periodic inundation of the area by basaltic lava flows and cinders. Individual flows range in thickness from 7 to 51 m. Long intervals of

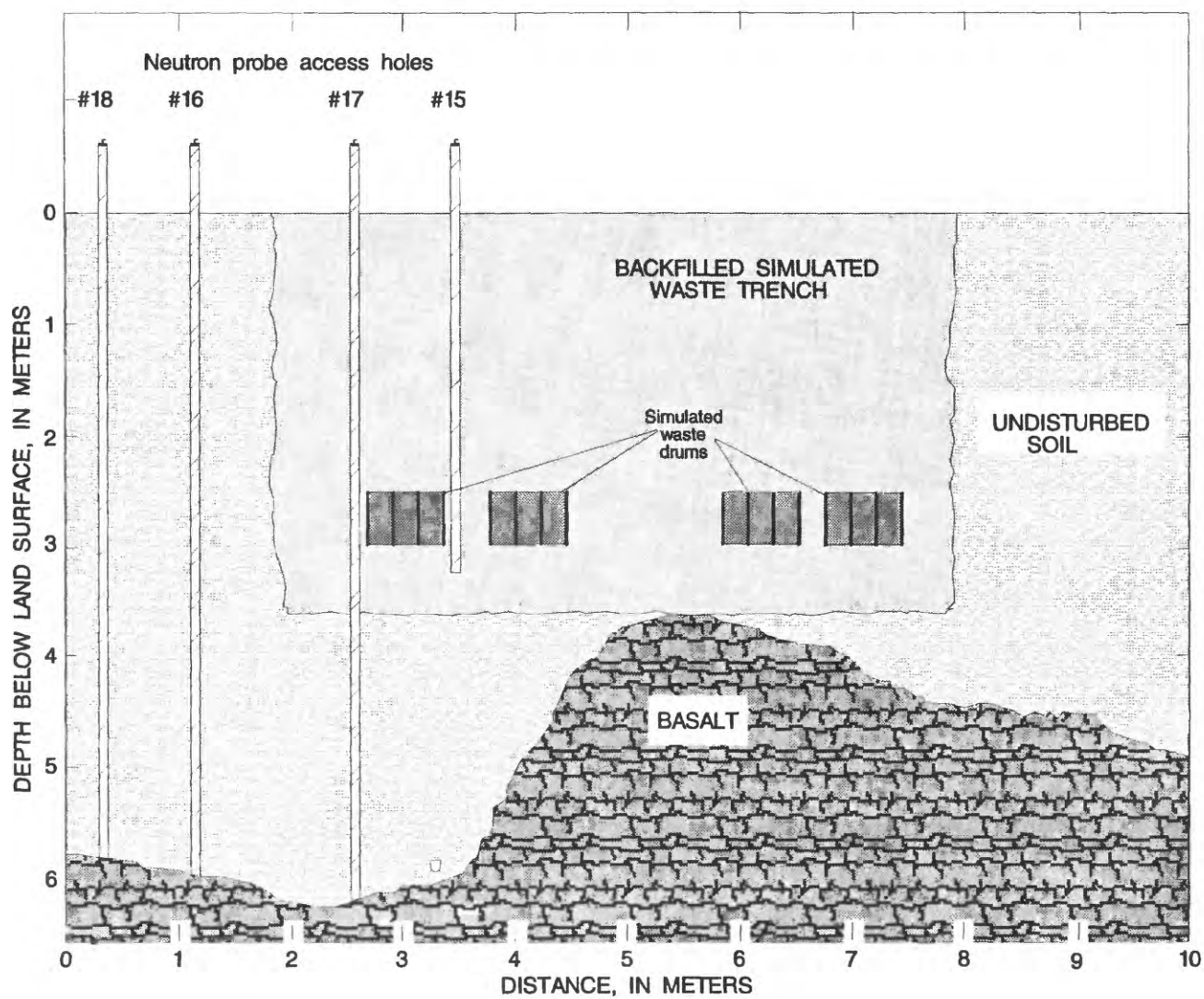


Figure 3. The simulated waste trench within the USGS test trench area, showing the excavated area and location of neutron-probe access holes. Stippled region shows area of excavation.

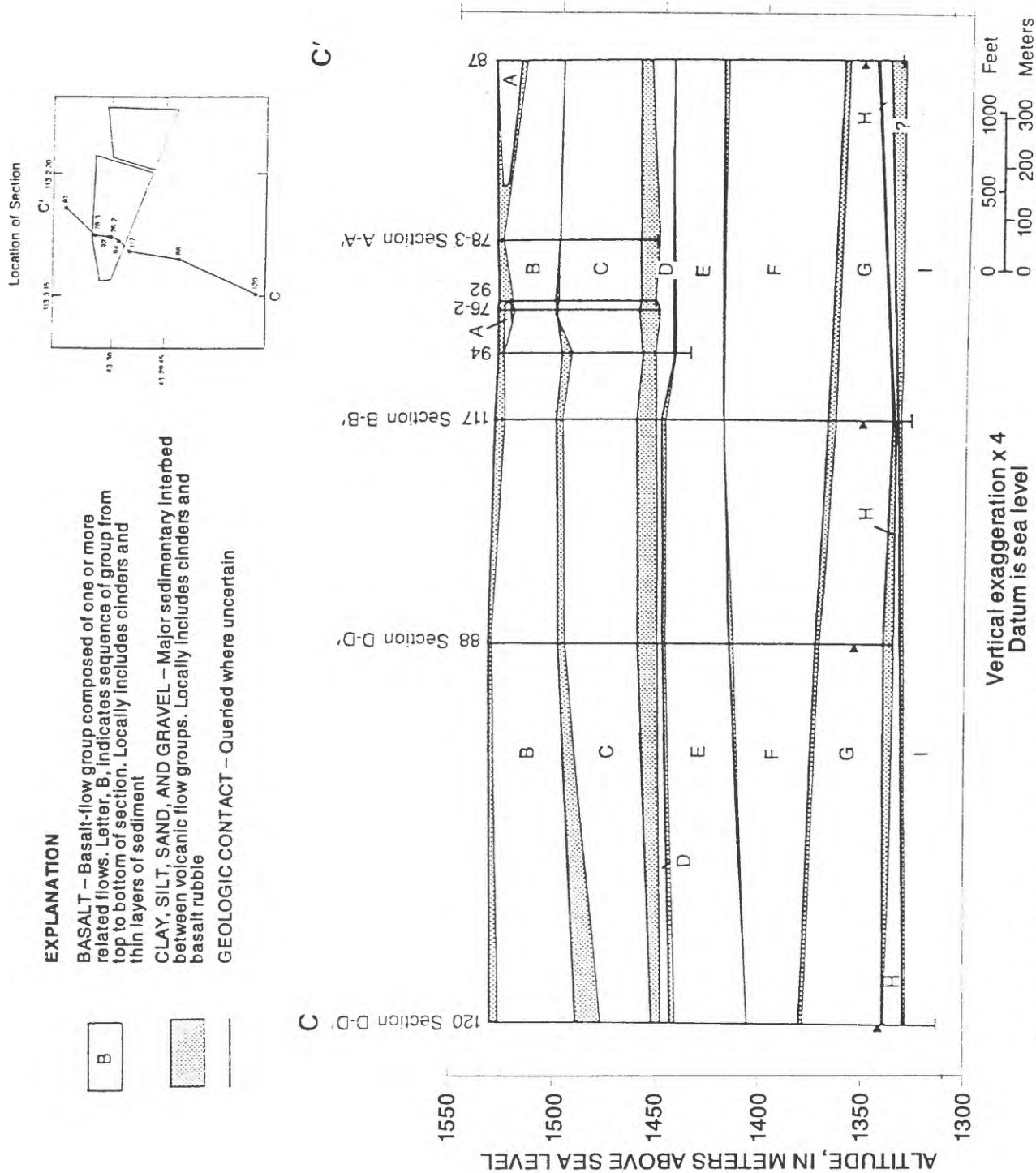


Figure 4. Subsurface geology at the Radioactive Waste Management Complex (Modified from Anderson and Lewis, 1989, p. 29).

volcanic inactivity were marked by the accumulation of sediment in stream channels, floodplains, playas, and dunes. The sedimentary sequences are discontinuous and vary in thickness from 0 to 12 m, averaging about 1.5 m. The thick sedimentary sequence between C and D, mostly silt and clay, is probably the remnant of a shallow lake.

The youngest flow sequence at the RWMC consists of one to two flows that erupted from Quaking Aspen Butte, about 19 km southwest of the RWMC, and flowed down the valley of the Big Lost River. The age of the flow sequence is $95,000 \pm 50,000$ years based on potassium-argon ratios (Anderson and Lewis, 1989).

Basaltic rock and intercalated sediment of the eastern Snake River Plain form the Snake River Plain aquifer, one of the world's largest aquifers. The aquifer is estimated to have a potential storage capacity of about 1 billion acre-feet of water. The aquifer is utilized extensively in agricultural, industrial, and domestic applications. At the RWMC, the depth to water is about 180 m. Groundwater flow is generally to the south-southwest, and hydraulic conductivities range from 1.5 to 6 m/day (Robertson and others, 1974).

Water movement in the unsaturated zone is driven mostly by gravitational and capillary forces. The matric potential (Ψ) in an unsaturated soil is a measure of the water pressure in the soil, which is negative. The gradient of this potential constitutes a driving force, as a result of which water flows from where total potential is higher to where it is lower. The matric potential depends on the soil-moisture content (θ), and increases as the soil-moisture content increases. Generally, at soil-moisture contents close to saturation, gravitational force dominates; however, as the soil dries, the matric potential gradient becomes much greater than the gravitational force. The nonlinear relationship between θ and Ψ is called a soil-moisture retention curve.

The amount of water retained at relatively high values of matric potential, between 0 and -1 atmosphere, depends primarily upon the pore-size distribution (Hillel, 1980). Effective pore size is commonly related to Ψ by the capillary equation:

$$\Psi = 2\gamma/r$$

where:

γ = surface tension between liquid and air
 r = pore radius

Therefore, as Ψ decreases, the largest pores empty out first, followed by progressively smaller pores.

When Ψ has decreased to the point where only the narrowest pores retain water, most of the water is held in hydration envelopes as adsorbed water, and the size and shape of pores have little influence. Therefore, the soil-moisture retention curves may be nearly identical for many soils in the low matric potential range (i.e., less than -1 atmosphere), where the predominant mechanism of water retention is adsorptive rather than capillary, and the retention capacity becomes more of a textural than a structural characteristic.

The hydraulic conductivity of an unsaturated soil depends on soil-moisture content. In a saturated soil all the pores are water filled and conducting and hydraulic conductivity is maximal. But, as the soil desaturates, the larger pores empty and become air filled, and flow is restricted to the interconnections between smaller and smaller water-filled pores. Thus, as the soil desaturates, tortuosity or actual flow-path length increases and hydraulic conductivity decreases.

Methods

During two site visits in June 1991 and August 1992, 35 soil-core samples for use in hydraulic-property studies were collected from 12 hand-augured bore holes at two locations within the USGS test trench area: (1) the undisturbed north-central part, and (2) the simulated waste trench area (fig. 5). Four samples from the 18-cm depth, collected by traditional hammering technique during an October 1990 site visit, also were used in this study.

During sample collection, some soil properties were changed irreversibly. Several mechanisms that resulted in disturbance during soil sampling have been identified (Gilbert, 1992):

- (1) Compression, extension, shear, and vibration from the intrusion of the sampling tube
- (2) Tension and shear from extraction of the tube

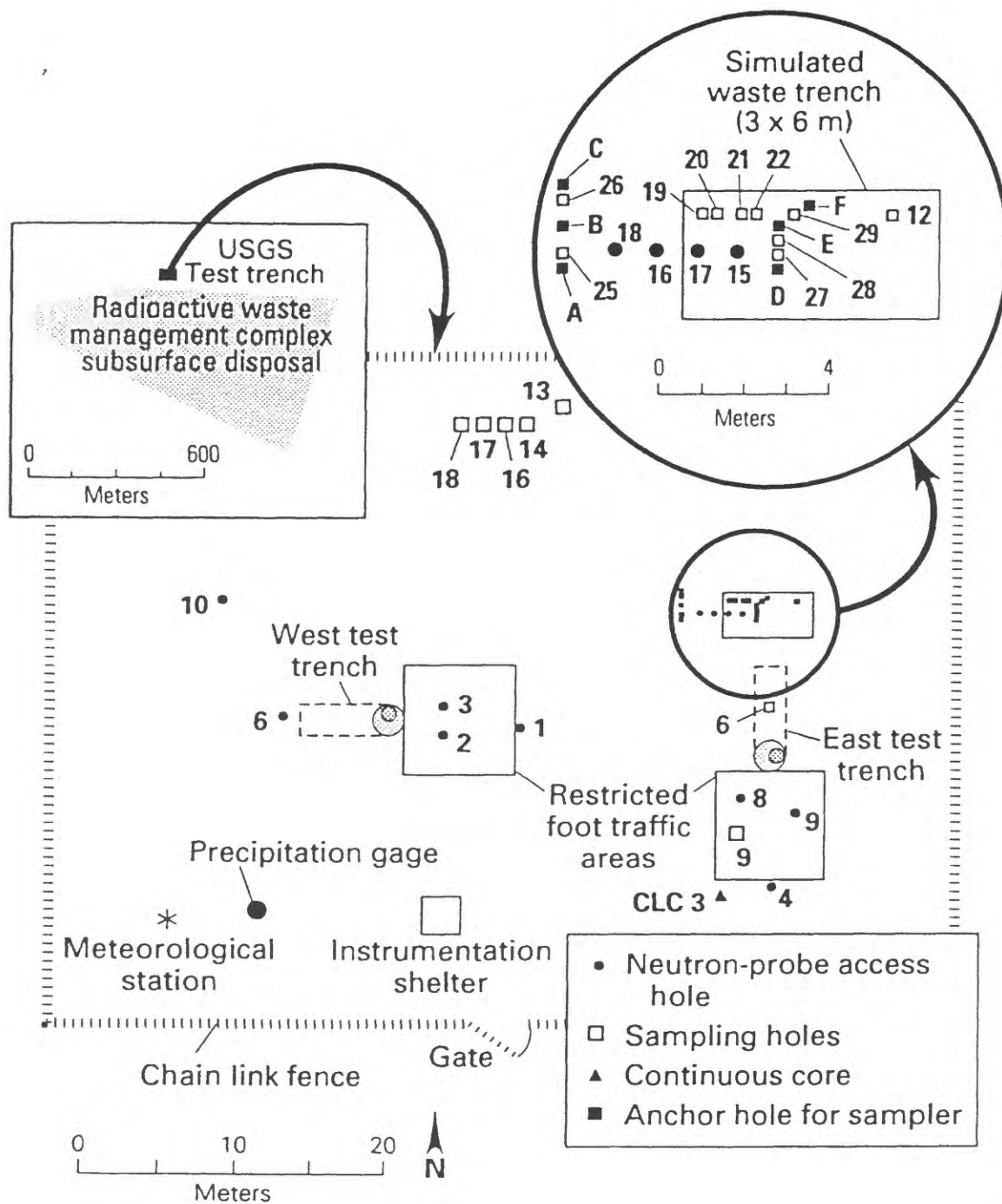


Figure 5. Location of the USGS test trench area, monitoring facilities, and soil-sample collection sites.

- (3) Shock and structural disturbance during transportation and storage
- (4) Compression, extension, shear, and vibration during extrusion and trimming operations.

Hydraulic conductivity measurements are particularly vulnerable to disruption caused by collection of the sample. Because the method of hydraulically pushing a sampler causes less disruption than other conventional methods such as hammering, samples for this study were collected with a thin-walled, hydraulically driven sampler. The sample cores were 5.1 cm in height and 5.0 cm in diameter. Sampling holes were hand-augured and sample cores were collected at intervals between 0.29- and 3.25-m depth. Samples then were trimmed, weighed, capped, and wrapped in aluminum foil to prevent moisture loss. The soil trimmings were retained for use in particle-size analysis.

It is well known that many soil structural features change during the various seasons of the year. Aggregation can deteriorate rapidly as the aggregates are subjected to seasonal precipitation, which causes slaking, swelling, shrinkage, and erosion. Because aggregate distribution is a dynamic property, this study evaluates and discusses only those differences observed between undisturbed and disturbed soils at the time of sampling.

Aggregate distribution and calcium carbonate content were determined in the field during sample collection in August 1992. A dry-sieve analysis method (Burke and others, 1986) was used to separate aggregates of different sizes. Samples used for analysis were collected from a hand-augered bore hole with a "riverside" auger. Approximately 1 kg of soil was collected then rotated in a series of nested sieves (4, 2, and 1 mm) for 3 minutes. Each aggregate fraction was then weighed. A qualitative index of calcium carbonate content was obtained by observing the reaction of the soil with 5-percent hydrochloric acid solution.

Particle-size analysis (PSA) was performed on all the samples using a Coulter LS100 Optical Particle Size Analyzer. This machine directs a beam of light through an aqueous suspension of the

particles and measures the diffracted light. An array of detectors measures how much light is scattered through various angles. The computer then calculates a particle-size distribution from the scattered light observed by the detectors.

Samples were sieved through a 1-mm sieve and then split using a spinning riffler. Approximately 0.3 g of sample was used for each measurement. In order to adequately disperse the soil, pretreatment of the sample included 15 minutes of sonication in an ultrasonic bath.

Additionally, because optical methods are not currently in wide use for soil application, four samples (two disturbed and two undisturbed) were also measured by the traditional pipette and sieving method (Gee and Bauder, 1986) for comparison with the optical method. The samples were measured once with sodium hexametaphosphate (HMP) pretreatment only, to deflocculate the clays, and again after the following pretreatments:

- (1) hydrogen peroxide washing to remove organics and carbonate,
- (2) centrifuging with distilled water to remove soluble salts, and
- (3) addition of HMP to deflocculate the clays.

Porosity was calculated from the bulk density measurement using a value of 2.65 g/cm^3 (Blake and Hartge, 1986) for particle density:

$$\text{Porosity} = 1 - (\text{bulk density} / \text{particle density})$$

The fundamental relationship of moisture content (θ) and matric potential (Ψ) was determined by means of a modified tension plate assembly: a submersible pressure outflow cell (SPOC) (Constantz and Herkelrath, 1984). Each sample was sealed in the SPOC apparatus and suspended in a bath of 0.005 mol/L of CaSeO and CaSO₄ to minimize biological growth and simulate a natural electrolyte balance. The samples were hung from an electronic balance that measured sample weight. Following saturation by wetting from the bottom up, pressure increments were applied. At each pressure increment, water was driven out of the sample until each sample met an equilibration criterion: change of sample weight less than or equal to 0.02 g in a 14-hour period. The applied air

pressure was equated to a matric potential after taking into account a correction for the submerged depth of the sample. The sample weights at equilibrium points were converted to moisture contents after samples were dried to a constant weight in an oven at 110° C and reweighed. The difference in weight measurements is equal to the moisture content on a dry-mass basis. Measurements were taken in the 0- to 1-atmosphere range where moisture retention is strongly influenced by the soil structure and where differences had been expected for a disturbed as opposed to undisturbed soil.

Saturated hydraulic conductivity (K_{sat}) was measured by a falling head method (Klute and Dirksen, 1986). K_{sat} measurements were performed immediately after the soil core was removed from the SPOC apparatus. The K_{sat} apparatus consisted of an open, cylindrical reservoir that was sealed with an O-ring to the top of the soil core sample. A stainless-steel filter on the bottom of the soil ring allowed for the outflow of solution while minimizing soil loss. When the cores were initially placed into the K_{sat} apparatus, their saturation was about 75 percent. Because complete saturation is necessary for the K_{sat} measurement, wetting the sample was accomplished with de-aired CaSeO and CaSO₄ solution (0.005 mol/L), allowing the sample to saturate from the bottom up for at least 24 hours. Then, the reservoir above the sample was filled carefully with de-aired selenate solution. As water flowed through the sample under the influence of gravity, the drop in water level was repeatedly measured using a depth gauge to an accuracy of ± 0.02 mm. K_{sat} measurements in the laboratory vary with time due to the changes in trapped air and growth of soil microorganisms (Christiansen, 1944; Allison, 1947). A minimum of six runs (a run being equivalent to one full reservoir, approximately 220 cm³ of solution, running through the soil core) was necessary to achieve a constant K_{sat} .

The unsaturated hydraulic conductivity ($K(\theta)$) values were generated using the one-step outflow method, a transient-flow method originally described by Gardner (1956). The one-step outflow method directly produced values of diffusivity, $D(\theta)$. $K(\theta)$ was then calculated using Ψ values from

the SPOC data and the equation:

$$K(\theta) = D(\theta) (d\theta/d\Psi).$$

The one-step outflow experiments were carried out at the end of the soil-moisture retention experiment while the samples were still in the SPOC apparatus. When the last equilibrium point was established for the soil-moisture retention curve, the sample was allowed to resaturate. Then, a positive air pressure of 1,000 cm of water was applied to the saturated sample and the change in sample weight was recorded as a function of time. $D(\theta)$ was calculated by the method of Passioura (1976).

PHYSICAL PROPERTIES OF SOIL

The purpose of describing the physical properties of a soil is to provide information which will better define the characteristics of the site and the soil. Better definition allows for a full interpretation of the site-specific hydrologic processes.

Soil Profile Description

A continuous core (CLC-3 on fig. 5) was drilled within the surficial sediments of an undisturbed area at the USGS test trench area in October 1990. Drilling was completed to a depth of 5.8 m before reaching basalt. Table 1 provides a description of the continuous core as described in August 1992.

Aggregate Distribution

The results of the dry sieving of the soil for determination of aggregate distribution, from both disturbed and undisturbed soils, are listed in table 2. While the sieve method used here is proposed for air-dry soil, the moisture content at the time of sampling was considered low enough (ranging from 14 to 30 percent) that the sieve analysis could be carried out in the field.

Carbonate Content

The results of the hydrochloric acid (HCl) test in the field are compiled in table 3. This method is

Table 1. Soil profile description

Horizon	Color (Munsell color chart)	Depth (cm)	Structure	Texture	Hydrochloric acid reaction
A	dark, yellowish, brown 10YR4/2	0-17	granular	sandy silt	none to moderate
Bk1	pale, yellowish, brown 10YR7/2	17-140	angular blocky (3-33mm), strong, coarse to fine	sandy silt	moderate to strong
2Bk2	pale, yellowish, brown 10YR7/2	140-164	angular blocky (3-33mm), coarse to fine	clayey silt 10% sand	moderate
2C	moderate, yellowish, brown 10YR5/4	164-295	subangular blocky (30mm), medium to coarse	sandy silt	moderate to slight
3C2	moderate, yellowish, brown 10YR6/2	295-453	massive (buried soil?)	clayey silt	none to slight

Table 2. Aggregate distribution

Hole ID	Depth (cm)	>4.0 mm	4.0-2.0 mm	2.0-1.0 mm	<1.0 mm
		Percent by weight			
Undisturbed					
Anchor A	17-23	12.2	18.7	13.3	55.8
Anchor A	33-38	3.07	13.4	12.0	44.0
Anchor A	41-48	34.5	12.3	12.2	41.1
Hole 25	78-85	22.5	14.5	14.4	51.4
Hole 25	120-126	23.6	15.7	13.9	46.7
Hole 25'	131-138	31.9	20.9	13.4	33.8
Hole 25	155-162	50.7	16.5	12.1	20.8
Hole 25	186-192	52.2	14.0	11.6	22.2
Hole 25	209-217	23.7	15.8	18.3	42.3
Hole 25	255-261	9.5	18.5	18.6	53.4
Hole 25	328-332	14.7	20.9	21.3	43.2
Disturbed					
Anchor D	20-30	17.9	10.8	11.4	59.9
Anchor D	37-45	17.4	13.4	14.0	55.2
Anchor D	50-59	18.4	12.0	13.7	56.0
Hole 28	55-62	16.4	14.3	14.3	55.0
Hole 28	79-87	17.0	13.7	15.0	54.4
Hole 27	123-134	20.4	16.8	14.7	48.1
Hole 28	158-163	26.4	16.5	15.7	41.4
Hole 28	187-197	31.7	15.3	15.6	37.4
Hole 29	211-219	32.6	17.4	15.1	34.8
Hole 27	348-357	45.2	17.9	13.7	23.2

Table 3. Reaction between soil and hydrochloric acid

Undisturbed (Anchor A)						Disturbed (Hole 28)					
Depth (cm)	None	None to moderate	Moderate	Moderate to strong	Strong	Depth (cm)	None	None to moderate	Moderate	Moderate to Strong	Strong
17	X					15			X		
23		X				28					X
29					X	40					X
38					X	50					X
64					X	77					X
75					X	87					X
88					X	104					X
129					X	129					X
153				X		141					X
169				X		153					X
178			X			175					X
198					X	206					X
206					X	284				X	
242		X									
250		X									
265		X									
280		X									
302		X									
310	X										
337	X										

Table 4. Particle-size distribution by method

Sample	Depth (cm)	Sieve & pipette (HPM only)			Sieve & pipette (pretreated)			Optical method (Sonication only)		
		% Sand	% Silt	% Clay	% Sand	% Silt	% Clay	% Sand	% Silt	% Clay
Undis- turbed	75	34.1	51.3	14.6	34.3	48.8	16.9	29.7	51.3	19.1
Undis- turbed	27	26.2	56.3	17.4	19.6	60.1	20.4	25.4	56.4	18.2
Disturbed	79	21.2	60.3	18.5	19.2	60.9	19.8	21.3	58.4	20.3
Disturbed	29	34.2	51.3	14.6	29.8	51.6	18.6	28.4	52.5	19.2

considered to be moderately subjective and qualitative and is used here only as an indicator of carbonate content. The strong reaction to HCl in samples from the 29- and 129-cm depths in the undisturbed profile supports the description of the B_k horizon in the continuous core (table 1). The disturbed profile has a much more uniform HCl reaction profile.

Particle-Size Analysis

Comparison between the sieve and pipette method and the optical method showed only small differences in particle sizes as seen in table 4. Sieve and pipette analysis performed by Laney and Minkin (1988) at the INEL showed similar results for undisturbed samples from about the same location and depth in the test trench area. Figure 6 shows the particle-size distribution with depth for the disturbed soils of the simulated waste trench and the adjacent undisturbed area, for data obtained by the optical method only.

HYDRAULIC PROPERTIES OF SOIL

The purpose of describing the hydraulic properties of a soil is to allow for a full interpretation of the site-specific hydrological processes. The hydraulic properties described include: soil-moisture retention, saturated hydraulic conductivity, and unsaturated hydraulic conductivity.

Soil-Moisture Retention Curves

The soil-moisture retention curves are plotted by depth in figure 7. The most extreme differences between disturbed and undisturbed soil cores appear at the 235-cm depth. The undisturbed cores at this depth show large porosities and gradual slopes in their soil-moisture retention curves. However, it appears that the disturbance, resulting in a small increase in porosity but a large increase in the number of larger pores, produced a substantially steeper curve

Saturated Hydraulic Conductivity

The results of the K_{sat} experiments are shown in figure 8. The change in conductivity decreased and the values stabilized after approximately 6 runs or 27 pore volumes of solution were passed through the soil (a volume of about 220 cm^3 solution per run flowing through a sample with an average soil volume of 100 cm^3 and an average porosity of 0.50). The increase of K_{sat} with time and the eventual constant value obtained presumably were due to the removal of entrapped air and a decrease in microbial activity.

Unsaturated Hydraulic Conductivity, $K(\theta)$

Figure 9 compares $K(\theta)$ plots from the transient one-step outflow method for disturbed and undisturbed cores with depth. The K_{sat} reported is the value of the final run of the data in figure 8. A comprehensive listing of measured soil properties and sample holes and numbers is presented in table 5. The field θ values reported for samples that were not artificially wetted during sampling are computed from sample weight at time of collection and oven-dry weight.

DIFFERENCES IN PHYSICAL AND HYDRAULIC PROPERTIES OF DISTURBED AND UNDISTURBED SEDIMENTS

Figure 10 shows a distribution with depth of relative carbonate content, clay content, moisture content from neutron probe data collected at time of sampling, porosity, aggregates, and K_{sat} for both the undisturbed soil and the disturbed soil from the simulated waste trench. Distinct horizon development is seen in the undisturbed profile. The most noteworthy feature in the profile of the simulated waste trench is the homogeneity of the soil. The absence of the natural layers is evident from the relatively smooth profiles of the relative carbonate content, clay content, and aggregate distribution in the disturbed simulated waste trench.

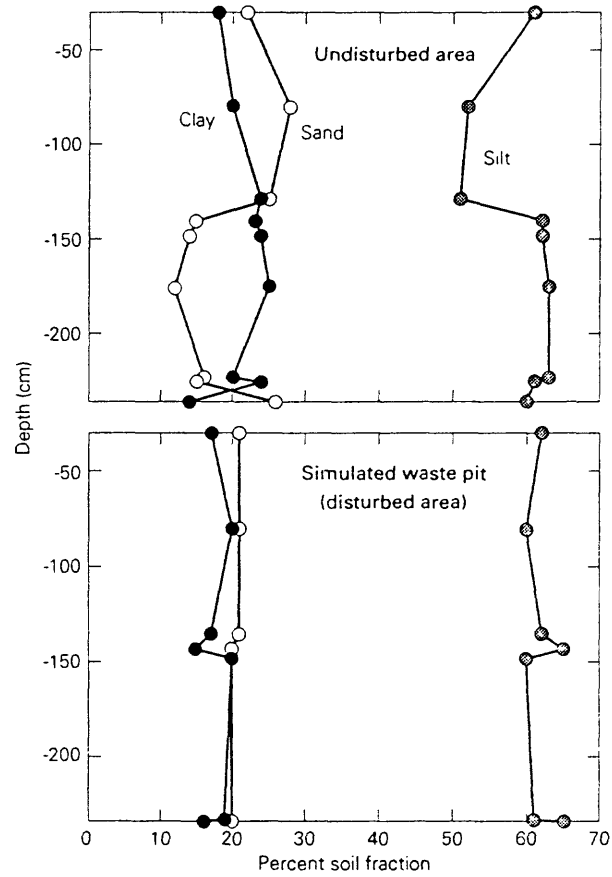


Figure 6. Particle-size distribution with depth in the undisturbed area and the simulated waste trench at the USGS test trench area.

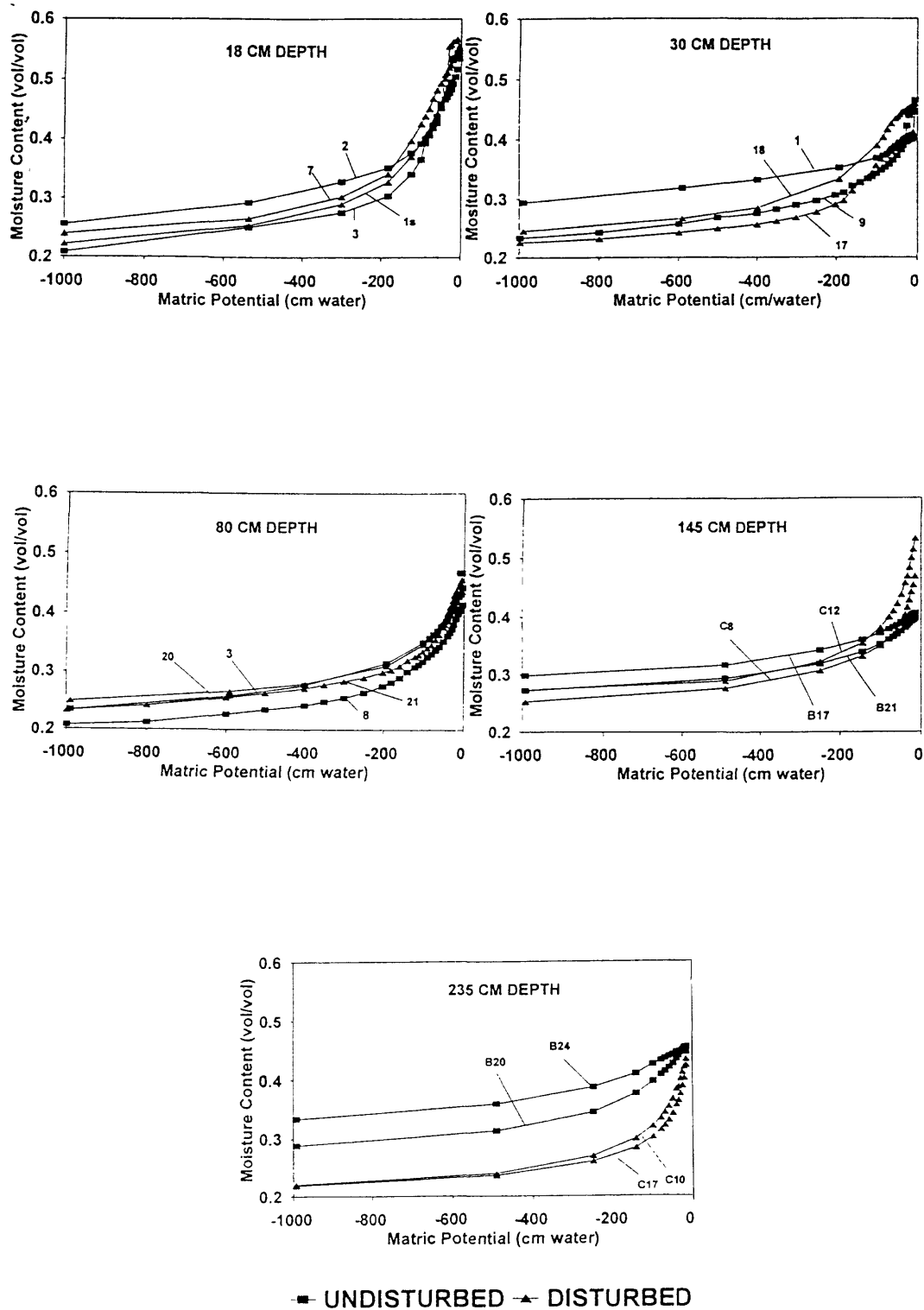


Figure 7. Soil-moisture retention curves plotted by depth for sediment samples in the undisturbed area and simulated waste trench at the USGS test trench area.

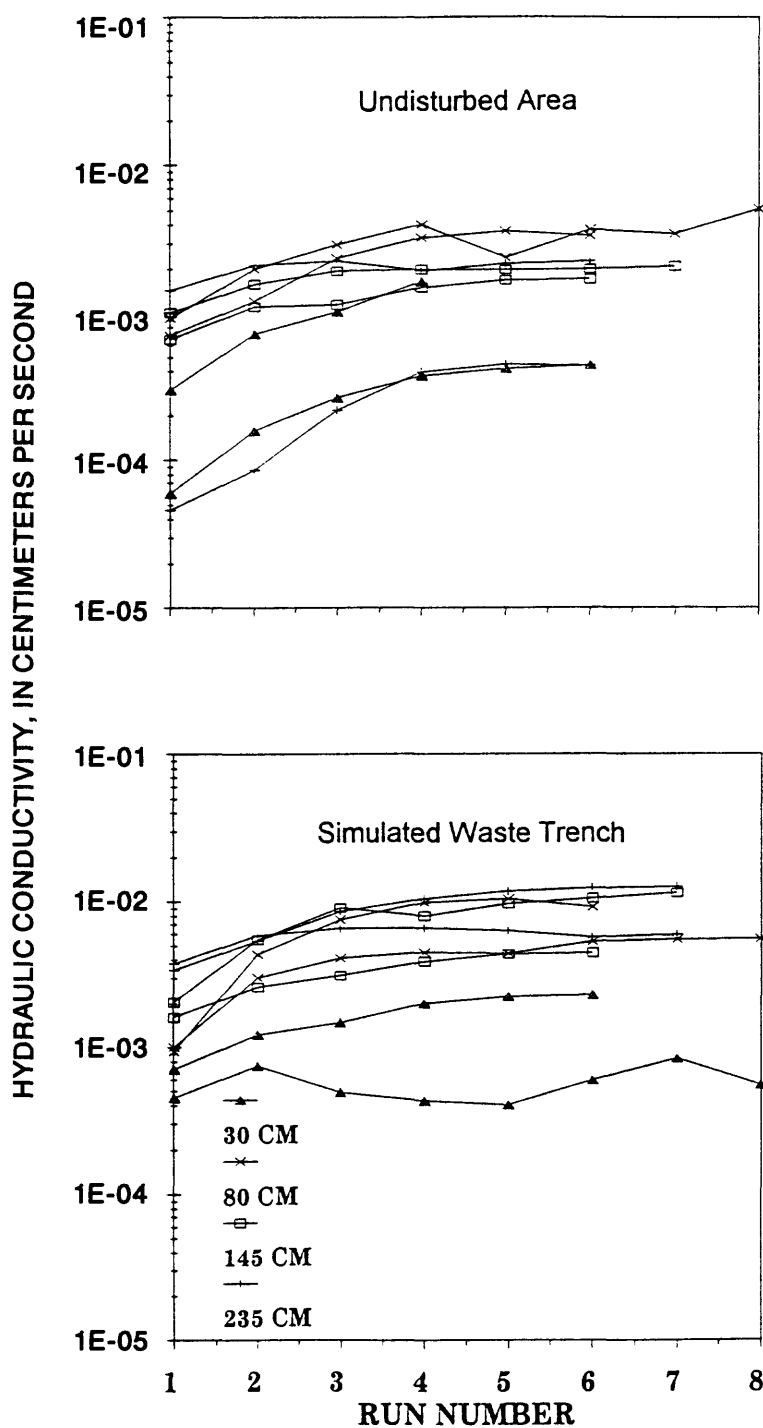


Figure 8. Saturated hydraulic conductivity variation in the undisturbed area and the simulated waste trench with number of experimental runs, USGS test trench area.

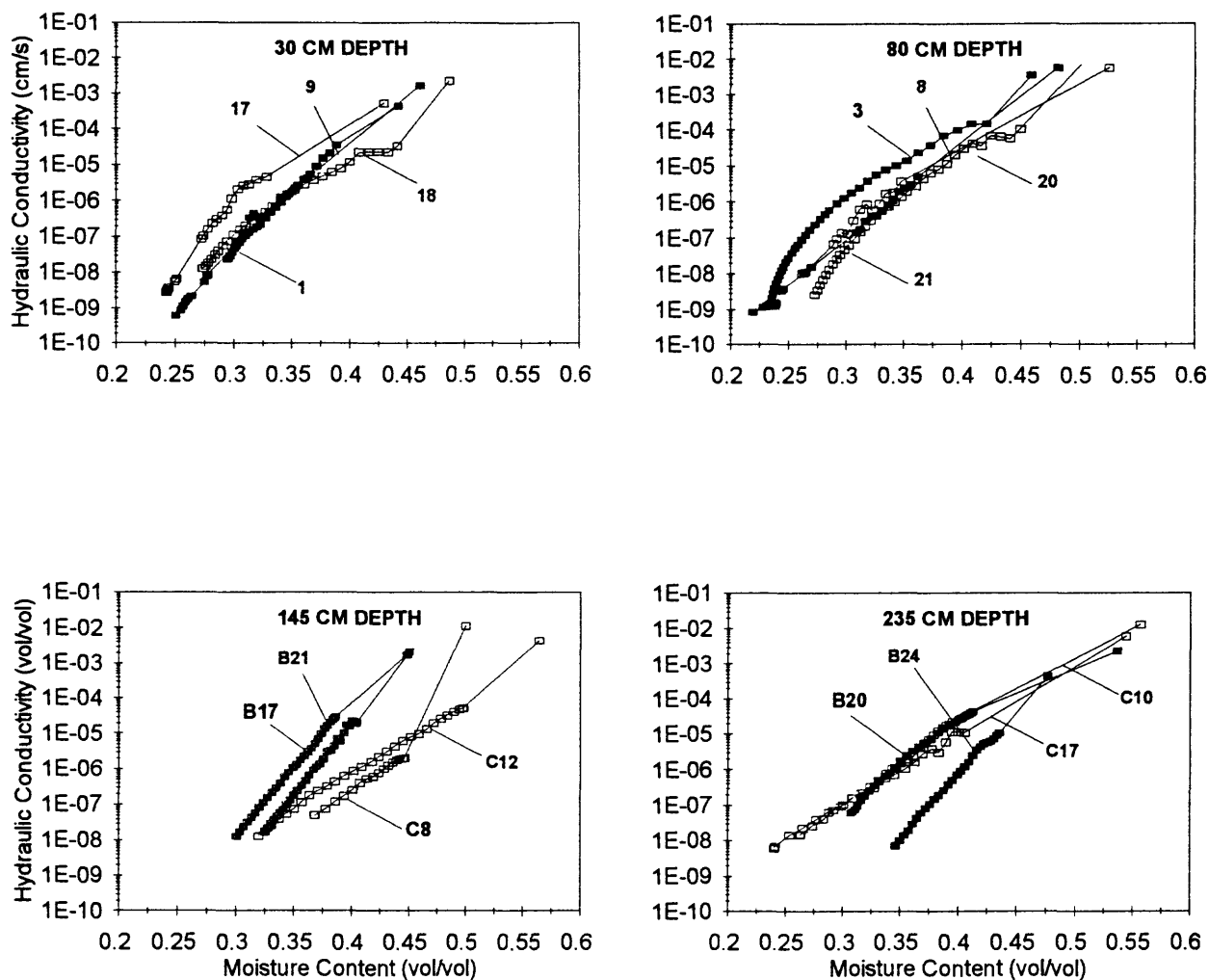


Figure 9. Unsaturated hydraulic conductivity curves with saturated hydraulic conductivity, plotted by depth in the undisturbed area and the simulated waste trench at the USGS test trench area.

Table 5. Summary of soil properties

Hole number	Sample number	Depth (cm)	Bulk density (g/cm ³)	Percent clay	Field moisture content (θ)	Porosity	Saturated hydraulic conductivity (cm/s)
Undisturbed							
9	2	18	1.40	13.7	.1052	.4716	--
13	3	18	1.39	--	.1752	.4746	--
17	9	27	1.43	18.2	.1478	.4615	1.6x10 ⁻³
14	1	33	1.48	17.7	--	.4424	4.4x10 ⁻⁴
14	8	75	1.37	19.1	.1412	.4821	5.5x10 ⁻³
16	3	80	1.43	20.2	--	.4589	3.3x10 ⁻³
16	4	129	1.46	24.1	.1827	.4497	2.6x10 ⁻³
26	B21	140	1.46	22.6	--	.4510	2.1x10 ⁻³
25	B17	148	1.46	24.1	--	.4490	1.7x10 ⁻³
16	5	175	1.41	25.1	.2725	.4691	5.6x10 ⁻⁴
26	B24	223	1.39	20.1	--	.4766	4.4x10 ⁻⁴
16	6	225	1.25	23.9	.2620	.5299	2.1x10 ⁻³
25	B20	226	1.23	14.2	--	.5367	2.3x10 ⁻³
Disturbed							
12	1s	18	1.31	15.5	.2010	.5015	--
6	7	18	1.24	14.8	.1247	.5294	--
21	17	29	1.52	19.2	.2264	.4299	5.5x10 ⁻⁴
22	18	29	1.36	20.8	--	.4869	2.3x10 ⁻³
22	21	79	1.26	20.3	--	.5254	5.5x10 ⁻³
21	20	79	1.31	20.6	--	.5044	9.2x10 ⁻³
19	14	135	1.19	21.3	.1664	.5505	--
29	C12	147	1.39	20.4	--	.5640	4.4x10 ⁻³
27	C8	148	1.33	19.8	--	.5001	1.2x10 ⁻²
27	C10	223	1.21	19.5	--	.5441	6.0x10 ⁻³
29	C17	237	1.18	19.3	--	.5567	1.3x10 ⁻²

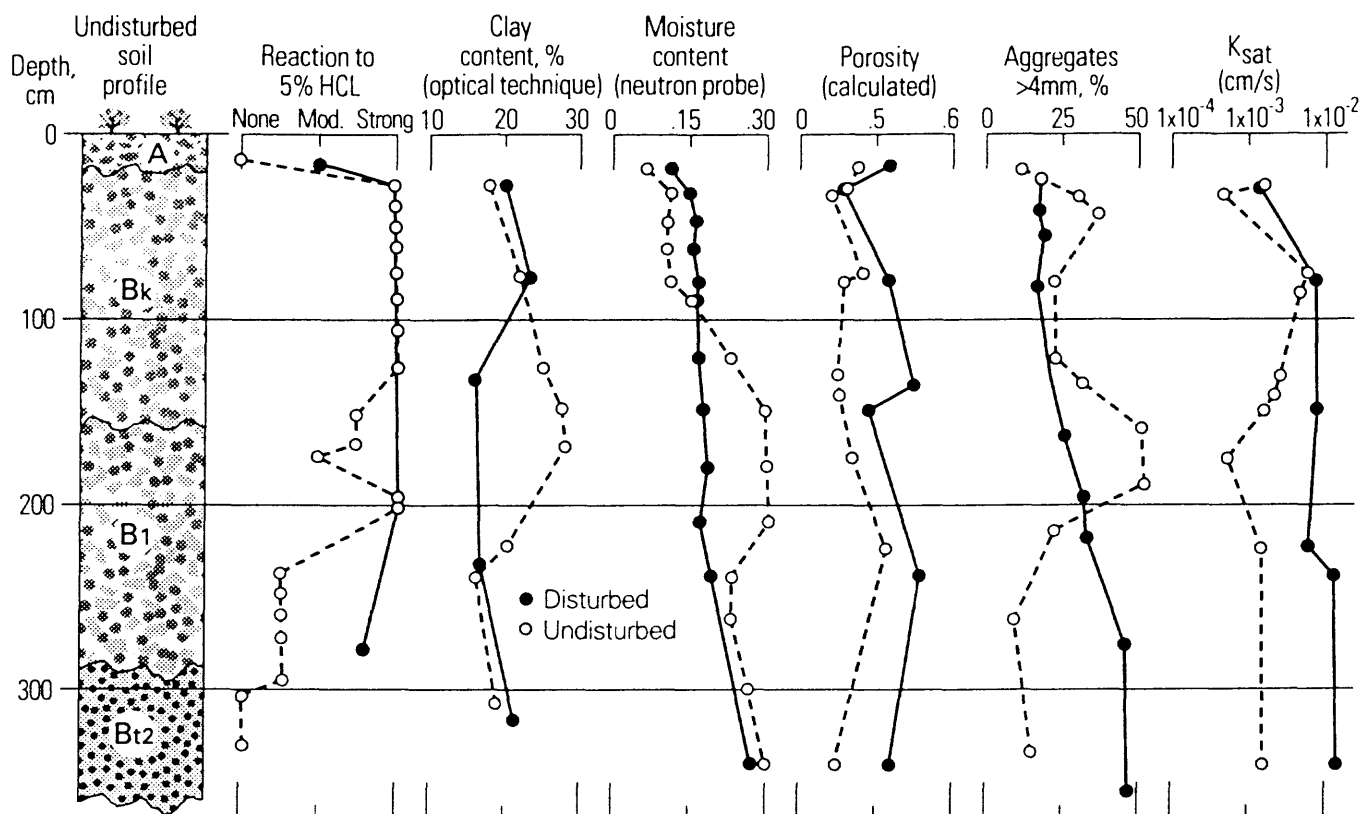


Figure 10. Compositing distribution of soil properties in a silt loam soil for undisturbed and simulated waste trench profiles at the USGS test trench area.

The calcic horizon described from the continuous core at the depth interval of 17-164 cm was confirmed in the field by the HCl test (table 3). The increase in clay content at the 140-220 cm depth interval, from samples collected in the undisturbed area, was not observed in the continuous core. It is not surprising, though, that the finger assessment method used for determining soil texture from the continuous core would not allow for the discernment of the 10- to 20-percent increase in clay content. After microbial gum, the most important constituent in the formation of aggregates is clay content; hence, the increase in clay is possibly the main factor responsible for the increase in aggregation (table 2) at similar depths.

The moisture content data plotted in figure 10 were collected at the time of sampling from neutron probe number 18 in the undisturbed area and neutron probe number 15 (fig. 5) in the disturbed soil from the simulated waste trench (Pittman, unpublished data). The increase in soil-moisture content between the 140-220-cm depth is most likely the result of the increase in clay content.

An inverse relationship between aggregates >4 mm and K_{sat} can be discerned in the profile of undisturbed soil shown in figure 10. The increase in large aggregates at a depth of 140 to 220 cm most likely is being controlled by the increase in clay; because of the higher clay content, K_{sat} is smaller at this depth even with the increase in large aggregates.

What is most discernible about the disturbed soil in the simulated waste trench is the destruction of the original horized profile. The clay content, carbonate profile, and aggregate distribution are more uniform through the disturbed profile than they are in the undisturbed profile. As a result, soil-moisture content is uniform with depth. Construction of the simulated waste trench has essentially created an unlayered, homogenized soil of unconsolidated sediments with increases in porosity of as much as 5 percent due to “fluffing” or “loosening” of the soil.

The heterogeneity of the undisturbed soil and homogeneity of the disturbed soil also are apparent in the soil-moisture retention curves (fig. 11). At the driest point on the curves, where $\psi = -1,000$ cm of

water, the soil-moisture contents range from 21 to 34 percent for the undisturbed soils. Lateral heterogeneity is also apparent, because samples from the same depths are from different sampling holes ranging from about 1 to 30 m apart. For the undisturbed cores at $\psi = -1,000$, the soil-moisture contents differ by as much as 6 percent at the 30-cm depth and by as little as 2.5 percent at the 145-cm depth. The soil-moisture retention curves for the samples of disturbed soil are strikingly similar in shape and the soil-moisture contents at the driest point, $\psi = -1000$, vary between 22 and 28 percent, less than half of the range for the undisturbed samples. Additionally, the lateral heterogeneity, apparent in the undisturbed cores, is diminished in the cores from disturbed soil, which differ in moisture content at $\psi = -1000$ by a maximum of 2.8 percent at the 30-cm depth and by a minimum of 0.3 percent at the 235-cm depth.

It is well known that disturbing a soil by “fluffing” or “loosening” will tend to decrease bulk density and increase total porosity. Several studies have also shown that soil disturbance will destroy macroporosity (Ehlers, 1975; Warner and Nieber, 1991; Roseberg and McCoy, 1991). What was observed in these studies was that, in the disturbed soils, the destruction of insect burrows and rootlet channels yielded an overall decrease in macroporosity, while still showing an increase in porosity. Pore-size distributions for this study were calculated from the soil-moisture retention curve data based on the capillary equation $r = 2\gamma/(-\psi)$, where r = pore radius, and γ = surface tension of the soil solution, which is estimated at 67 mN/m based on studies by Chen and Schnitzer (1978) and Tschapek and others (1978). The cores from disturbed soil show an increase in frequency of pore sizes for the range of ψ measured as shown in figure 12. Although pore sizes greater than 0.13 mm could not be measured, it is possible that the observed increase in pore sizes in the cores from disturbed soil, shown in figure 12, is a result of the destruction of larger pores and their replacement by smaller-sized pores. This interpretation could also help to explain the $K(\theta)$ relationships.

The $K(\theta)$ relationships in disturbed and undisturbed soils are plotted in figure 13. The linear regression of $\log K$ shows that the unsaturated

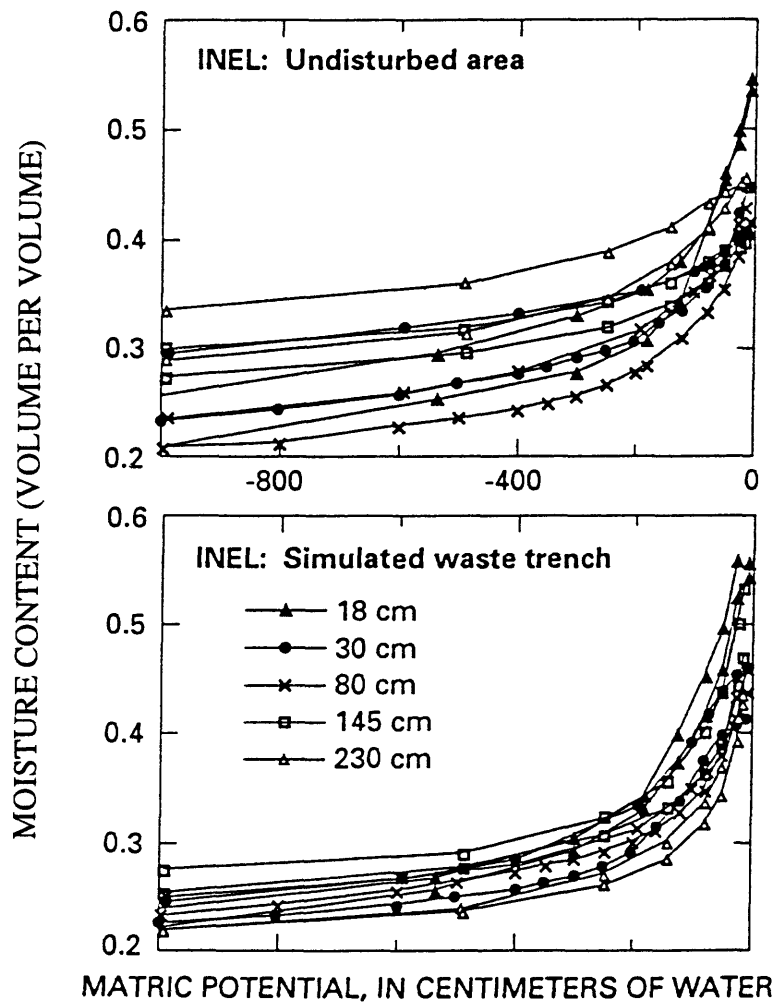


Figure 11. Soil-moisture retention curves for disturbed and undisturbed soils at the simulated waste trench, USGS test trench area.

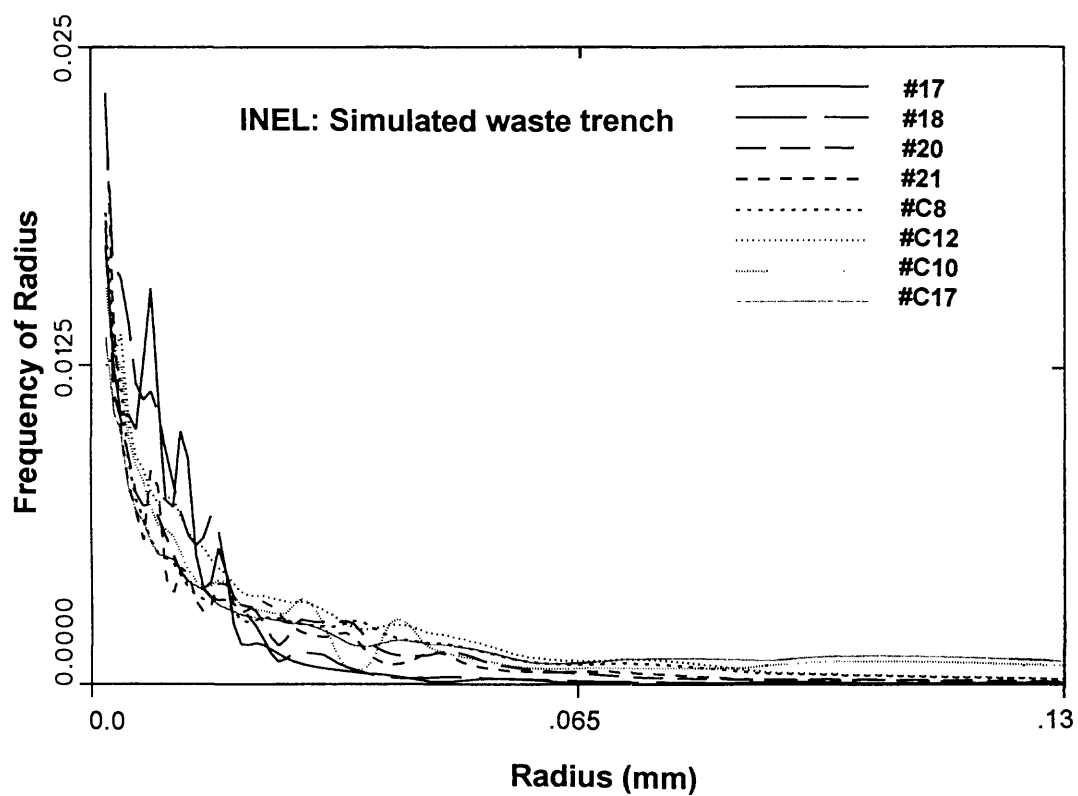
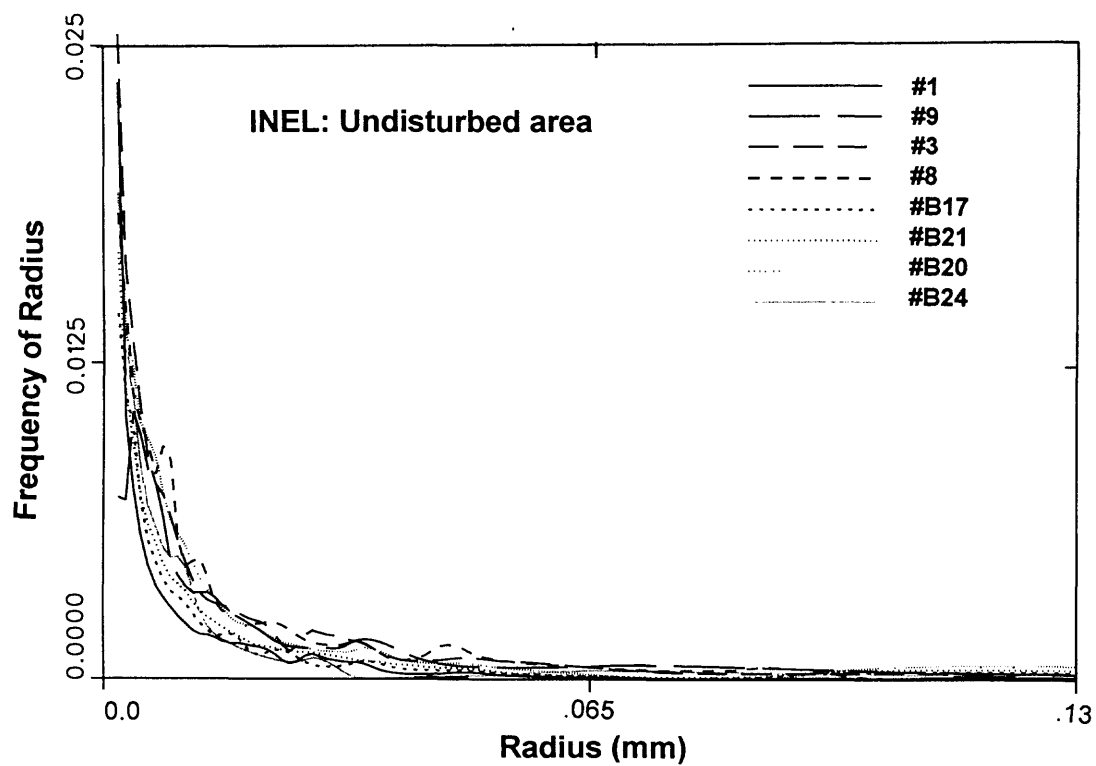


Figure 12. Frequency distribution of effective pore sizes in disturbed and undisturbed soils at the simulated waste trench, USGS test trench area.

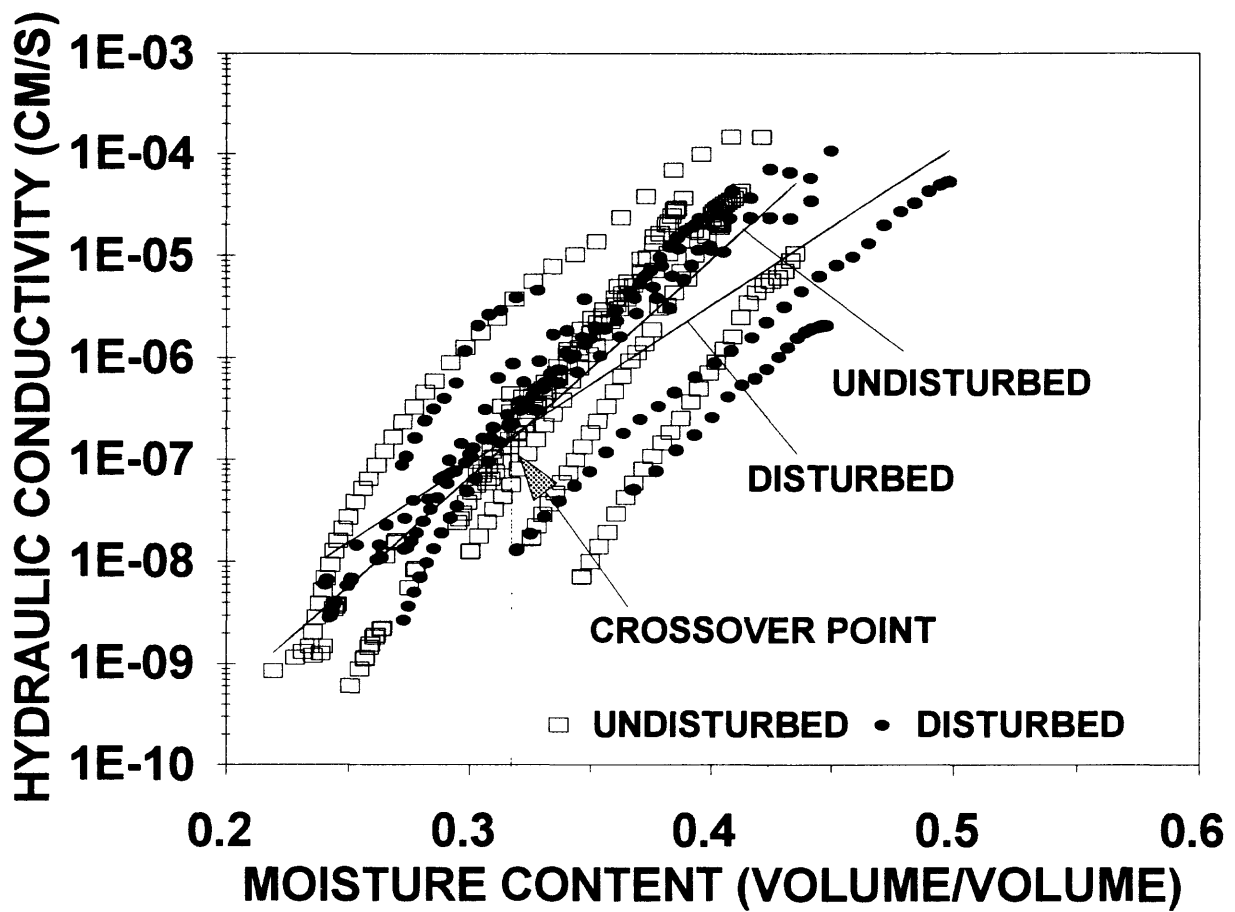


Figure 13. $K(\theta)$ curves for disturbed and undisturbed soils at the simulated waste trench, USGS test trench area.

hydraulic conductivity of undisturbed soil on average is higher than that of the disturbed soil at moisture contents above 32 percent. At lower moisture contents, there is a tendency for the disturbed soil to have higher conductivity. This effect might be expected based on the lack of large pores in the disturbed soil. The loss of large pores and channels will decrease conductivity at higher moisture contents. However, the resultant increase in smaller pores will have the effect of increasing the conductivity at lower moisture contents. This result is consistent with the data of other studies on disturbed versus undisturbed loamy soils (Ehlers, 1977; Allmaras and others, 1977; Jayawardane and Prathapar, 1992).

SUMMARY AND CONCLUSIONS

Based on laboratory and field measurements, substantial differences exist between the physical and hydraulic properties of the undisturbed and the disturbed soils at the simulated waste trench. The profile of the undisturbed soil shows distinct layers, or horizons, with a high clay content layer at a depth of 140 to 220 cm. These layers are homogenized to a large degree in the profile of disturbed soil which contains relatively uniform mixtures of carbonate, clay, moisture, and aggregates. The porosity and K_{sat} typically are larger at each depth for samples from disturbed soil than for samples from undisturbed soil.

Soil-moisture retention curves obtained from disturbed soil in the simulated waste trench show less vertical and lateral heterogeneity within the profile than do curves obtained from the corresponding undisturbed soil. In the disturbed soil, a slight decrease in θ results in a sharp decrease in measured K . This decrease in K may be a result of the emptying of intermediate-size pores created during soil disturbance. At lower moisture contents, the hydraulic conductivity of the disturbed soil will be greater than that of the undisturbed soil.

In undisturbed soil next to the simulated waste trench, the high clay content layer between about 140 and 220 cm depth probably restricts vertical flow. More water may remain above this depth, increasing evapotranspiration losses. In contrast, the destruction of the original layered profile in the

disturbed soil of the simulated waste trench probably increases vertical flow. Therefore, the trench may have wetter soil in the 3-6 m zone in which the simulated waste is buried.

Additionally, the higher the K_{sat} of a soil, the higher the rate of infiltration tends to be. When conditions are drier ($\theta < 0.32$), which is the case most of the year in eastern Idaho, downward percolation is greater in the disturbed soil because $K(\theta)$ is greater for this moisture range.

SELECTED REFERENCES

- Allison, L.E., 1947, Effect of microorganisms on permeability of soil under prolonged submergence: *Soil Science*, v. 63, p. 439-450.
- Allmaras, R.R., Rickman, R.W., Ekin, L.G., and Kimball, B.A., 1977, Chiseling influences on soil hydraulic properties: *Soil Science Society of America Journal*, v. 41, p. 796-803.
- Anderson, S.R. and Lewis, B.D., 1989, Stratigraphy of the unsaturated zone at the Radioactive Waste Management Complex, Idaho National Engineering Laboratory, Idaho: U.S. Geological Survey Water-Resources Investigations Report 89-4065, 22 p.
- Blake, G.R., and Hartge, K.H., 1986, Particle density, in Klute A., *Methods of soil analysis, Part I: American Society of Agronomy, Soil Science Society of America, Madison, Wis.*, p. 377-382.
- Burke, W., Gabriels, D., and Bouma, J., 1986, Soil structure assessment: A.A. Balkema, Rotterdam, Netherlands, p. 30-31.
- Chen, Y., and Schnitzer, M., 1978, The surface tension of aqueous solutions of soil humic substances: *Soil Science*, v. 125, p.7-15.
- Christiansen, J.E., 1944, Effect of entrapped air upon the permeability of soils: *Soil Science*, v. 58, p. 355-365.

- Clawson, K.L., Start, G.E., and Ricks, N.R., 1989, *Climatography of the Idaho National Engineering Laboratory*, 2nd edition: U.S. Department of Energy Report DOE/ID-12118, 115 p.
- Constantz, J., and Herkelrath, W.N., 1984, An improved pressure outflow cell for measurement of pore water properties from 0 to 10° C: *Soil Science Society of America Journal*, v. 48, p. 7-10.
- Davis, L.C., and Pittman, J.R., 1990, Hydrological, meteorological, and geohydrological data for an unsaturated zone study near the Radioactive Waste Management Complex, Idaho National Engineering Laboratory, Idaho, 1987: USGS Open-File Report 90-114, p. 6-21.
- Ehlers, W., 1975, Observations on earthworm channels and infiltration on tilled and untilled loess soil: *Soil Science* v. 110, p. 242-249.
- Ehlers, W., 1977, Measurement and calculation of hydraulic conductivity in horizons of tilled and untilled loess-derived soil: *Geoderma*, v. 19, p. 293-306.
- Gardner, W.R., 1956, Calculation of capillary conductivity from pressure plate outflow data: *Soil Science Society of America Proceedings*, v. 20, p. 317-320.
- Gee, G.W., and Bauder, J.W., 1986, Particle-size analysis, *in* Klute, A., *Methods of soil analysis, Part I: American Society of Agronomy, Soil Science Society of America, Madison, Wis.*, p. 383-411.
- Gilbert, P.A., 1992, Effect of sampling disturbance on laboratory-measured soil properties: Department of the Army, Corps of Engineers, Miscellaneous Paper GL-92-35, 45 p.
- Hillel, D., 1980, *Fundamentals of soil physics*: Academic Press, New York, p. 123-162.
- Humphrey, T.G., Smith, T.H., and Pope, M.C., 1982, Projected subsurface migration of radionuclides from buried INEL trans-uranic waste: *Nuclear Technology*, v. 58, p. 136-149.
- Jayawardane, N.S., and Prathapar, S.A., 1992, Effect of soil loosening on the hydraulic properties of a duplex soil: *Australian Journal of Soil Research*, v. 30, p. 959-975.
- Klute, A., 1982, Tillage effects on hydraulic properties of a soil: A Review, *in* 'Predicting Tillage Effects on Soil Physical Properties and Processes: American Society of Agronomy Special Publication No. 44, Soil Science Society of America, Madison, Wis.', p. 29-43.
- Klute, A., and Dirksen, C., 1986, Hydraulic conductivity and diffusivity, laboratory methods, *in* Klute, A., *Methods of soil analysis, Part I: American Society of Agronomy, Soil Science Society of America, Madison, Wis.*, p. 687-732.
- Laney, P.T., and Minkin, S.C., 1988, Subsurface investigations program at the Radioactive Waste Management Complex of the Idaho National Engineering Laboratory: Annual Progress Report FY 1987, DOE/ID-10183, 150 p.
- Passioura, J.B., 1976, Determining soil water diffusivities from one-step outflow experiments: *Australian Journal of Soil Research*, v. 15, p. 1-8.
- Pittman, J.R., Jensen, R.G., and Fischer, P.R., 1988, Hydrologic conditions at the Idaho National Engineering Laboratory, 1982 to 1985: U.S. Geological Survey Water-Resources Investigations Report 89-4008, 70 p.
- Pittman, J.R., 1989, Hydrological and meteorological data for an unsaturated zone study near the Radioactive Waste Management Complex, Idaho National Engineering Laboratory, Idaho, 1985 and 1986: U.S. Geological Survey Open-file Report 89-74, 24 p.

- Rightmire, C.T., and Lewis, B.D., 1987, Hydrogeology and geochemistry of the unsaturated zone, Radioactive Waste Management Complex, Idaho National Engineering Laboratory, Idaho: U.S. Geological Survey Open-File Report 76-717, p. 1-22.
- Robertson, J.B., Schoen, R., and Barraclough, J.T., 1974, The influence of liquid waste disposal on the geochemistry of water at the National Reactor Testing Station, Idaho, 1952-1970: U.S. Geological Survey Open-File Report IDO-22053, 231 p.
- Roseberg, R.J., and McCoy, E.L., 1991, Crop and tillage induced changes in macropore geometry, *in* Preferential Flow: Proceedings of National Symposium, American Society of Agricultural Engineers, p. 383-392.
- Tschapek, M., Scoppa, C.O., and Wasowski, C., 1978, The surface tension of soil water: *Journal of Soil Science*, v. 29, p. 17-21.
- Warner, G.S., and Nieber, J.L., 1991, Macropore distributions in tilled vs. grass-surfaced cores as determined by computed tomography, *in* Preferential Flow: Proceedings of National Symposium, American Society of Agricultural Engineers, p. 192-201.